

# Warpage of a Large-Sized Orthogonal Stiffened Plate Produced by Injection Molding and Injection Compression Molding

Sung Hee Lee,<sup>1</sup> Seong Yun Kim,<sup>2</sup> Jae Ryoun Youn,<sup>2</sup> Baek Jin Kim<sup>1</sup>

<sup>1</sup>Precision Molds and Dies Team, Korea Institute of Industrial Technology, Songdo-Dong, Yeonsu-Gu, Incheon 406-840, Korea

<sup>2</sup>Department of Materials Science and Engineering, Research Institute of Advanced Materials (RIAM), Seoul National University, Sillim-Dong, Gwanak-Gu, Seoul 151-744, Korea

Received 9 July 2009; accepted 27 November 2009

DOI 10.1002/app.31873

Published online 22 February 2010 in Wiley InterScience (www.interscience.wiley.com).

**ABSTRACT:** Rectangular plates of the size of  $1800 \times 600 \times 12 \text{ mm}^3$  and  $1200 \times 600 \times 12 \text{ mm}^3$  were selected for injection molding and injection compression molding, respectively, in order to investigate warpage characteristics of the large-sized polymer plates with orthogonal stiffener. To determine the mold system and to reduce warpage of the specimen, numerical analyses for injection molding and injection compression molding were performed by using a commercial simulation code. Experiments were performed to verify the suggested mold system and warpage of the specimen. Relatively large warpage of the injection molded product was observed

and small warpage of the injection compression molded product was generated. Compression force of the injection compression molding was only 6% of the clamp force of the injection molding. Warpage of the product was reduced significantly by using the injection compression molding. The injection compression molding will be used to substitute expensive and disused wood forms with inexpensive and recyclable polymer plates for concrete casting. © 2010 Wiley Periodicals, Inc. *J Appl Polym Sci* 116: 3460–3467, 2010

**Key words:** molding; plastics; simulations; stress

## INTRODUCTION

Wooden plates are generally used as concrete forms in public works. Recently, two types of the forms such as euro-form and single body form are widely used. Euro-forms are inexpensive but all the used materials are disused after 7–8 usages. On the contrary, single body forms can be used for 30–40 times and recycled but its price is 10 times as expensive as that of the euro-forms.<sup>1</sup> Hence, inexpensive and recyclable materials for the forms in public works have been required. Recyclable and cheap polymeric materials are paid attention to because the forms can be manufactured by the relatively fast and cheap injection molding process. However, shrinkage of an injection molded polymeric product is inevitable because molten polymers are filled in the mold cavity and cooled

during injection molding cycles. Shrinkage of polymeric materials during injection molding depends on the kind of polymer materials and is generally lower than 5% of the cavity volume.<sup>2</sup>

Although shrinkage of the polymeric material is considered for design of the mold cavity, warpage can be generated if nonuniform in-mold shrinkage generated in thickness or in-plane direction because volumetric shrinkage of the material is simply considered for the mold design. Warpage of injection molded products are influenced by many parameters such as material properties, part geometry, tooling and injection molding conditions, etc.<sup>3</sup> Warpage causes numerous problems such as distortion of the finished part, difficulties in satisfying the target dimensions, higher internal stresses, etc. In especial, warpage frequently occurs in the cases of large-sized injection molded products and flat-molded articles because nonuniform in-mold shrinkage is easily generated due to the geometric effect. Therefore, precision control of the part shrinkage should be required in order to satisfy dimensional accuracy of the molded products. Although many studies on warpage of injection molded products have been reported,<sup>4–7</sup> there are few studies on warpage of large-sized orthogonal stiffened plastic plates.

Injection compression molding, combination of conventional injection molding and compression

Correspondence to: J. R. Youn (jaeryoun@snu.ac.kr).

Contract grant sponsor: Korea Institute of Industrial Technology (KITECH) and Korea Science and Engineering Foundation (KOSEF) grant funded by the Korean Government (MEST) through the Intelligent Textile System Research Center (ITRC); contract grant number: R11-2005-065.

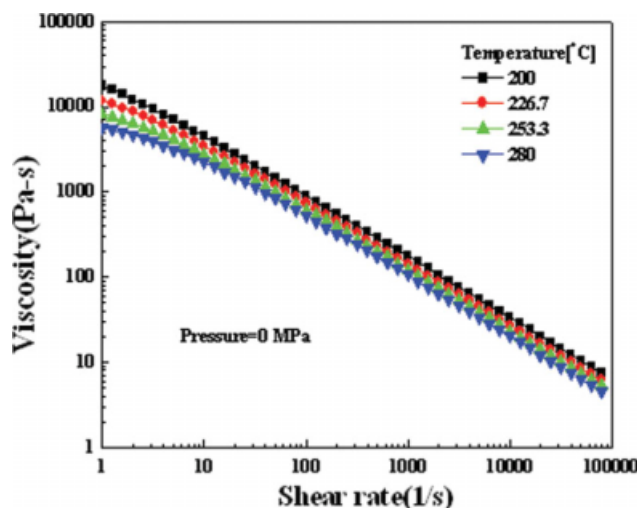


**Figure 1** Viscosity variation of the Thermocomp MEV-1006 with respect to shear strain rate at 200°C, 226.7°C, 253.3°C, and 280°C. [Color figure can be viewed in the online issue, which is available at [www.interscience.wiley.com](http://www.interscience.wiley.com).]

molding, was developed to incorporate the advantages of both molding processes. The compression stage can be introduced after partial filling of the cavity. It can also be activated to replace the packing and holding stages of the conventional injection molding. When compared with the typical injection molding, injection compression molding has such advantages as decreasing molding pressure, reducing residual stress, decreasing uneven shrinkage and warpage, and increasing dimensional accuracy. Because of these advantages, injection compression molding can be recommended to avoid the disadvantages of injection molding.<sup>8–11</sup>

The purpose of this study is to reduce warpage of the large-sized orthogonal stiffened plastic plate with many ribs. Orthogonal stiffened plastic plate specimens with the size of 1800 mm × 600 mm × 12 mm and 1200 mm × 600 mm × 12 mm in length, width, and total thickness were prepared, respectively, in order to investigate warpage of the injection molded and injection compression molded products. Ribs of 3 mm thickness were attached on the plate in order to improve bending stiffness of the structure. According to the Ref. 12, bending stiffness of the honeycomb structure is the highest but mold manufacturing and injection molding processability of the structure are poor and expensive. Bending stiffness of the orthogonal rib structure is the second highest and injection molding processability is excellent. In addition, the tooling cost of the latter is much less than that of the former. Consequently, the orthogonal rib structure is selected in this study. Warpage and optimum processing conditions of the injection and injection compression molding were obtained by numerical flow analysis

using Moldflow<sup>TM</sup> (6.0 version, Moldflow Pty. Ltd, Victoria, Australia). Warpage for the product was measured experimentally and the measurement results were compared with the numerical predictions.

## EXPERIMENTAL

### Materials and characterization

Glass fiber reinforced polypropylene (PP/GF, Thermocomp MEV-1006, LNP Engineering Plastic, USA) containing 30 wt % glass fibers was used for injection and injection compression molding of large-sized orthogonal stiffened plastic plates. Viscosity and PVT properties of the PP/GF resin were obtained because those of the polymer resin were the most important properties for flow analysis. Rheological properties of the polymer resin were measured by Moldflow lab in the shear rate range of 1–100,000 s<sup>-1</sup> at 200°C, 226.7°C, 253.3°C, and 280°C. PVT relation of the resin was also measured by Moldflow lab at the temperature range of 25–290°C at 0, 50, 100, 150, and 200 MPa. Shear viscosity and pressure–viscosity–temperature (PVT) properties of the resin were shown in Figures 1 and 2 with respect to the shear rate and pressure, respectively. Typical shear thinning behavior was observed and nondifferentiable PVT properties ranging from 175°C to 200°C was those of typical semi-crystalline polymers.

### Injection molding and injection compression molding

The PP/GF resin was dried at 80°C in vacuum for 4 h before injection and injection compression molding

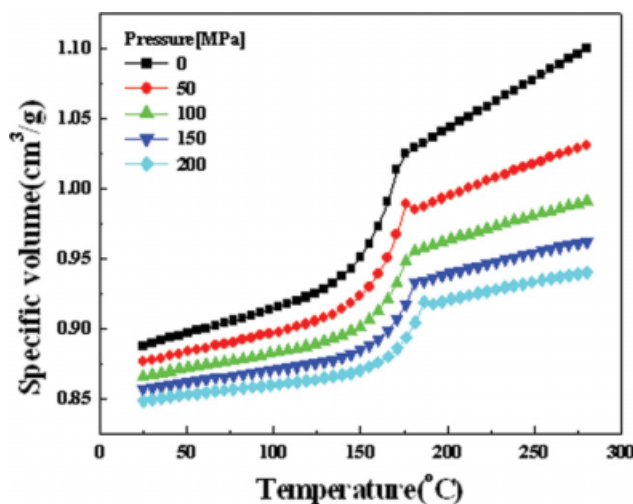


**Figure 2** Specific volume of the Thermocomp MEV-1006 with respect to temperature at 0, 50, 100, 150, and 200 MPa. [Color figure can be viewed in the online issue, which is available at [www.interscience.wiley.com](http://www.interscience.wiley.com).]

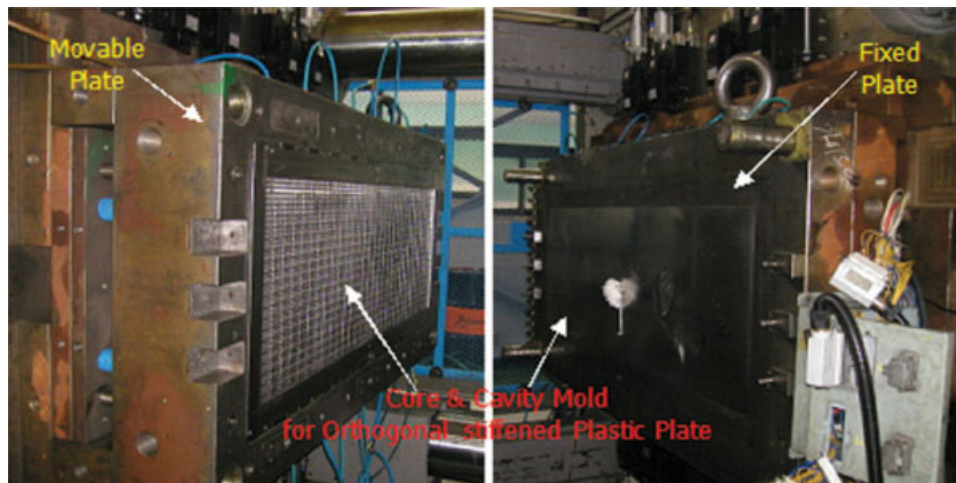


**Figure 3** Experimental setup for injection molding of large-sized orthogonal stiffened plastic plate. [Color figure can be viewed in the online issue, which is available at [www.interscience.wiley.com](http://www.interscience.wiley.com).]

to minimize the effect of moisture. Large-sized orthogonal stiffened plastic plates of the size of  $1800 \times 600 \times 12 \text{ mm}^3$  and  $1200 \times 600 \times 12 \text{ mm}^3$  were molded by using an injection molding machine [DIMA1050 TON (screw diameter: 150 mm, maximum injection pressure:  $1316 \text{ kg/cm}^2$ , maximum injection rate:  $8.8 \text{ cm/s}$ ), Dongshin Hydraulics co., Busan, Korea]. An injection compression molding machine [ID 3000 HM (screw diameter: 615 mm, maximum injection pressure:  $1356 \text{ kg/cm}^2$ , maximum injection rate:  $30 \text{ cm/s}$ ), LS Mtron, Jeollabuk-Do, Korea] was also used to produce orthogonal stiffened plastic plates. Experimental setup of the injection and injection compression molding for large-sized orthogonal stiffened plastic plates are shown in Figures 3 and 4 and molding conditions of both methods are listed in Table I. In the case of the injection compression molding, the mold was installed in a typical press and polymer resin was fed to the mold at the side as shown in Figure 4.

### Numerical flow simulation

The generalized Hele-Shaw model has provided relatively exact results for flow of molten polymer resin in a thin three-dimensional cavity. Governing equations for typical injection molding assuming inelastic, nonisothermal, and non-Newtonian fluid flow are as follows<sup>13–15</sup>:

$$\frac{\partial}{\partial z} \left( \eta \frac{\partial u}{\partial z} \right) - \frac{\partial p}{\partial x} = 0 \quad (1)$$

$$\frac{\partial}{\partial z} \left( \eta \frac{\partial v}{\partial z} \right) - \frac{\partial p}{\partial y} = 0 \quad (2)$$

$$\frac{\partial p}{\partial t} + \frac{\partial}{\partial x} (\rho u) + \frac{\partial}{\partial y} (\rho v) = 0 \quad (3)$$

$$\rho C_p(T) \left( \frac{\partial T}{\partial t} + u \frac{\partial T}{\partial x} + v \frac{\partial T}{\partial y} \right) = \frac{\partial}{\partial z} \left( k(T) \frac{\partial T}{\partial z} \right) + \eta \dot{\gamma}^2 \quad (4)$$

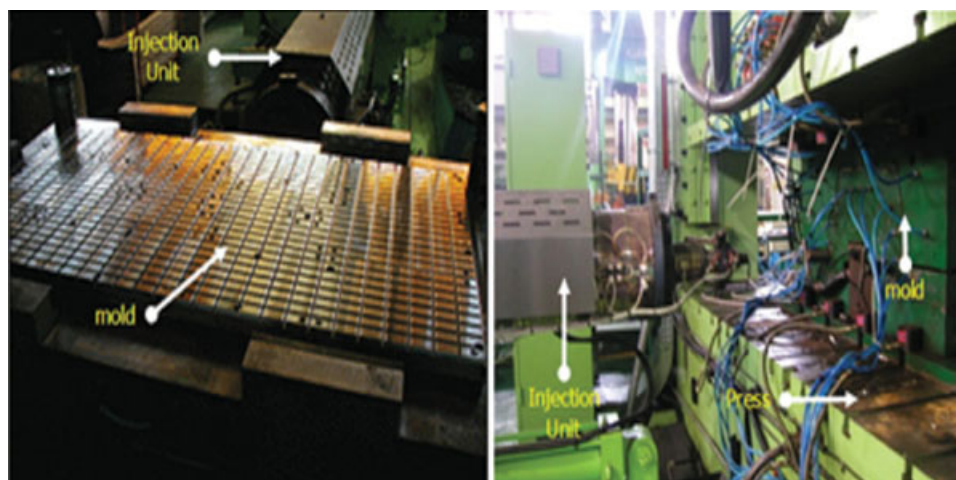


**Figure 4** Experimental setup for injection compression molding of large-sized orthogonal stiffened plastic plate. [Color figure can be viewed in the online issue, which is available at [www.interscience.wiley.com](http://www.interscience.wiley.com).]

**TABLE I**  
Processing Conditions for Injection and Injection Compression Moldings

|                            | Injection molding | Injection compression molding |
|----------------------------|-------------------|-------------------------------|
| Mold temperature (°C)      | 50                | 50                            |
| Melt temperature (°C)      | 240               | 240                           |
| Injection time (s)         | 8.5               | 5                             |
| Cooling time (s)           | 100               | 150                           |
| Compression delay time (s) | –                 | 6                             |
| Compression time (s)       | –                 | 20                            |
| Compression force (ton)    | –                 | 150–160                       |

$$\frac{\partial}{\partial x} \left( S \frac{\partial p}{\partial x} \right) + \frac{\partial}{\partial y} \left( S \frac{\partial p}{\partial y} \right) = G \frac{\partial p}{\partial t} + F \quad (5)$$

where,

$$S = \int_0^b \rho \int_z^b \frac{z}{\eta} dz d\bar{z} \quad (6)$$

$$G = \int_0^\delta \left( \frac{\partial \rho_l}{\partial p} \right)_r dz + \int_\delta^b \left( \frac{\partial \rho_s}{\partial p} \right)_r dz \quad (7)$$

$$F = \int_0^\delta \left( \frac{\partial \rho_l}{\partial T} \right)_p \frac{\partial T}{\partial t} dz + \int_\delta^b \left( \frac{\partial \rho_s}{\partial T} \right)_p \frac{\partial T}{\partial t} dz + (\rho_l - \rho_s)_{z=\delta} \frac{\partial \delta}{\partial t} \quad (8)$$

where,  $P$ ,  $T$ ,  $u$  and  $v$  represent pressure, temperature,  $x$  directional velocity of the molten polymer and  $y$  directional velocity of the molten polymer, respectively.  $\dot{\gamma}$ ,  $\eta$ ,  $p$ ,  $C_p$ , and  $k$  are shear rate, viscosity, density, specific heat under uniform pressure, and thermal conductivity, respectively. Non-Newtonian viscosity can be represented by the modified Cross model.<sup>13,16,17</sup>

$$\eta(T, \dot{\gamma}, p) = \frac{\eta_0(T, p)}{1 + (\eta_0(T, p) \dot{\gamma} / \tau^*)^{1-n}} \quad (9)$$

where,  $\eta$  is viscosity,  $\eta_0$  is the zero shear rate viscosity,  $\dot{\gamma}$  is shear rate,  $\tau^*$  is the shear stress at the transition between Newtonian and Power-law behavior, and  $n$  is Power-law index.  $\eta_0$  can be represented as a function of temperature by the Williams-Landel-Ferry (WLF) equation.

$$\eta_0(T, p) = D_1 \exp \left( - \frac{A_1(T - T^*(p))}{\bar{A}_2 + D_3 p + (T - T^*(p))} \right) \quad (10)$$

where,  $T^*(p) = D_2 + D_3 p$ . There are seven constants in eqs. (9) and (10), and the values of the Thermo-comp MEV-1006 are listed in Table II. The modified

Tait equation describes the PVT relationship of the polymeric material as below.

$$v(p, T) \begin{cases} (a_{0s} + a_{1s}(T - T_g)) \left( 1 - 0.0894 \ln \left( 1 - \frac{p}{B_s} \right) \right) & (T \leq T_g) \\ (a_{0m} + a_{1m}(T - T_g)) \left( 1 - 0.0894 \ln \left( 1 - \frac{p}{B_m} \right) \right) & (T > T_g) \end{cases} \quad (11)$$

where,

$$T_g = T_{g0} + B_2 p \quad (12)$$

$$B_m = B_{0m} e^{-B_{1m} T}$$

$$B_s = B_{0s} e^{-B_{1s} T}$$

$$C_p(T) = C_1 + C_2 \bar{T} + C_3 \tan h(C_4 \bar{T}) \quad (13)$$

$\bar{T} = T - C_s$  and  $C_1 - C_5$  are specific heat parameters. Convection heat transfer by cooling channels, heat conduction through the mold wall, and viscous heat generation during both filling and post-filling stages are accounted for in the thermal analysis. The coupled thermal and flow fields are solved with the control volume approach to handle automatic melt front advancement by using a hybrid FEM/FDM scheme. An implicit numerical scheme is used to solve the discretized energy equation.<sup>18</sup> Properties of the PP/GF resin (Thermocomp MEV-1006, LNP Engineering Plastic, USA) was used as properties of the resin for injection and injection compression moldings. Selected material properties for the polymer material are summarized in Table III and molding conditions for both numerical calculation and experiments were the same.

## RESULTS AND DISCUSSION

Preliminary prediction was performed in order to obtain optimum injection molding conditions by considering filling of the cavity.<sup>19-22</sup> High injection pressure was required due to large size and numerous ribs of the product and the high injection pressure can cause processing problems such as non-uniform pressure distribution and warpage. Gate, runner, and cooling channel system considered fluidity of the product is shown in Figure 5. Variation of the injection pressure at the nozzle is also shown with respect to injection time in Figure 5. The minimum injection pressure was obtained at the gate

**TABLE II**  
Constants of the Modified Cross Model with WLF Equation for the Thermo-comp MEV-1006

| $n$    | $\tau^*$ (Pa) | $D_1$ (Pa s) | $D_2$ (K) | $\frac{D_3}{(K/Pa)}$ | $A_1$  | $\bar{A}_2$ (K) |
|--------|---------------|--------------|-----------|----------------------|--------|-----------------|
| 0.2784 | 19,133        | 2.22e + 018  | 263.15    | 0                    | 39.013 | 51.6            |

**TABLE III**  
Material Properties of the Polymer Resin for Numerical Flow Simulation

| Properties                                       | Thermocomp MEV-1006                      |
|--|--|
| Melt density (kg/m <sup>3</sup> )                | 971.4                                    |
| Solid density (kg/m <sup>3</sup> )               | 1132.4                                   |
| Elastic modulus (MPa)                            | 5212                                     |
| Poisson's ratio                                  | 0.437                                    |
| Thermal expansion coefficient (K <sup>-1</sup> ) | 3.024E-5                                 |
| Specific heat (J/kg K)                           | 2407 (at 254.5°C, temperature dependent) |
| Thermal conductivity (W/m K)                     | 0.18 (at 215.5°C, temperature dependent) |

when injection time of about 8.5 sec was applied. When the injection time was used as stand point, shorter injection time caused higher injection pressure due to higher viscous effect of the polymer melt and longer injection time also caused higher injection pressure because of lower temperature of the polymer melt at the end of filling. Injection conditions that have been listed in Table I were determined based on the preliminary prediction.

Warpage of the large-sized orthogonal stiffened plastic plate observed by the experiment is shown in Figure 6 with numerically predicted results. Both results showed large warpage such that the surface without any rib was bent outward. The large warpage was attributed to thermal residual stresses developed in injection molding and the residual stresses are caused by nonuniform cooling of the large-sized product. Residual stress distribution in the thickness direction was predicted by the numeri-

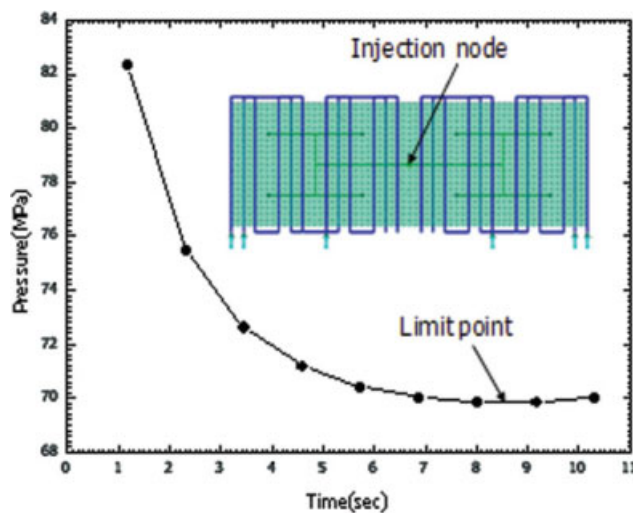


**Figure 5** Gate, runner, and cooling channel system of large-sized orthogonal stiffened plastic plate and injection pressure variation with respect to injection time. [Color figure can be viewed in the online issue, which is available at [www.interscience.wiley.com](http://www.interscience.wiley.com).]

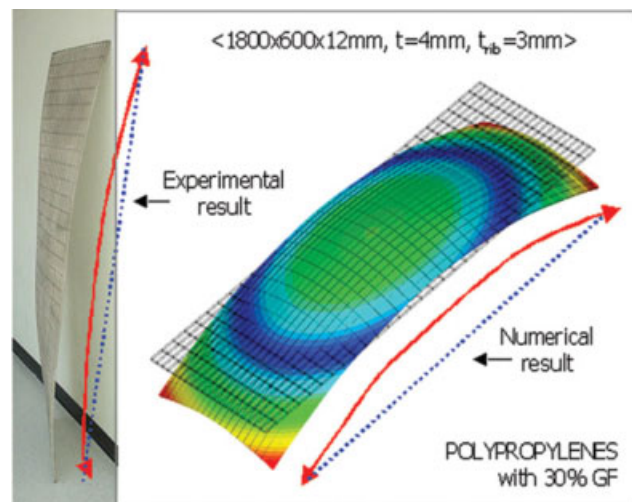


**Figure 6** Warpage of injection molded large-sized orthogonal stiffened plastic plate predicted by numerical simulation. [Color figure can be viewed in the online issue, which is available at [www.interscience.wiley.com](http://www.interscience.wiley.com).]

cal simulation and stresses of about 15–43 MPa were confirmed as shown in Figure 7. Pressure distribution lower than 100 MPa was also predicted at the end of filling but a large clamp force of about 2500 ton was required to produce the large-sized product. Thereafter, a very large injection molding machine was needed to carry out the production.

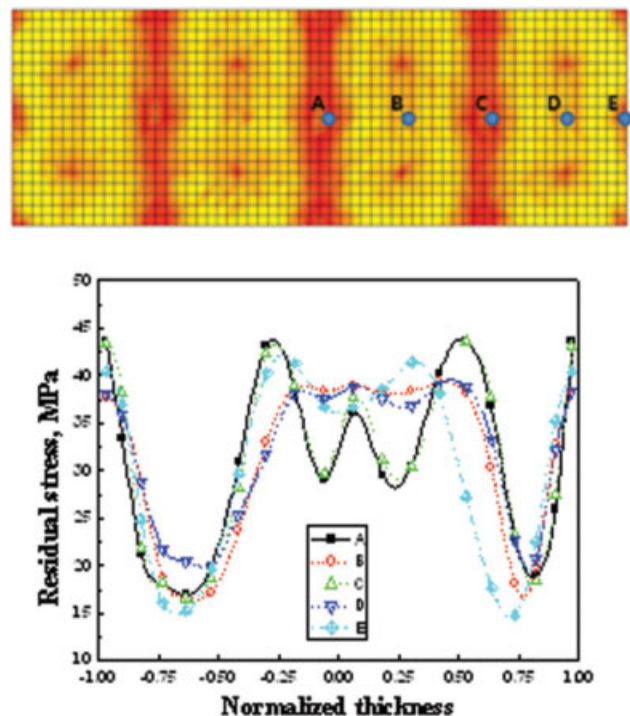


**Figure 7** Residual stress distribution of injection molded large-sized orthogonal stiffened plastic plate with respect to part thickness before ejection. [Color figure can be viewed in the online issue, which is available at [www.interscience.wiley.com](http://www.interscience.wiley.com).]

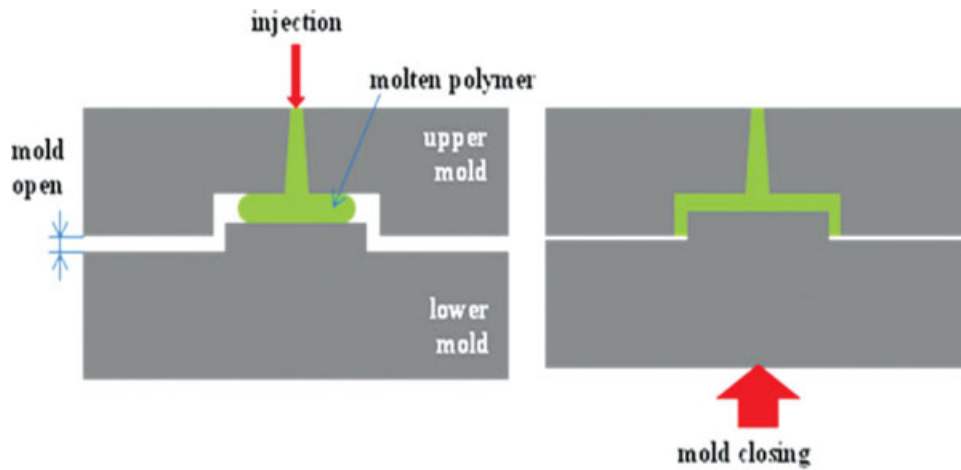


**Figure 8** Schematic diagram showing two stages of injection compression molding. [Color figure can be viewed in the online issue, which is available at [www.interscience.wiley.com](http://www.interscience.wiley.com).]

Because polymeric materials, an injection molding machine, and additional operations are selected by considering the property requirement of the end product at designing stage, changing the materials and processing conditions is impossible in many cases. Residual stresses should be minimized during injection molding in order to minimize warpage of the product. However, minimizing residual stresses of the product is limited because of relatively long flow path of the injected polymer melt in the case of large-sized products. Injection compression molding method was utilized in order to overcome the limitation of the injection molding. Schematic diagram of the injection compression molding is exhibited in Figure 8. The mold cavity is filled by the molten polymer resin and the final product is compression molded after closing the mold by applying the clamp force. Filling and packing pressure becomes

lower and the flow is shorter than those of the injection molding in the case of the injection compression molding, where uniform mold pressure is applied.

Preliminary numerical modeling was performed in order to determine number of gates before production of the mold for the injection compression molding. Three cases were considered for the prediction, that is, one gate, two gate, and three gate system. Flow advancements for the three cases are shown in Figure 9. Flow advancements for the

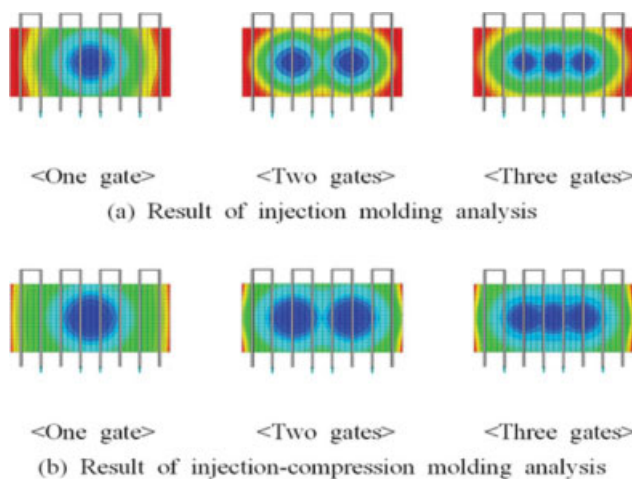


**Figure 9** Comparison of flow advancement between injection molding and injection compression molding. [Color figure can be viewed in the online issue, which is available at [www.interscience.wiley.com](http://www.interscience.wiley.com).]

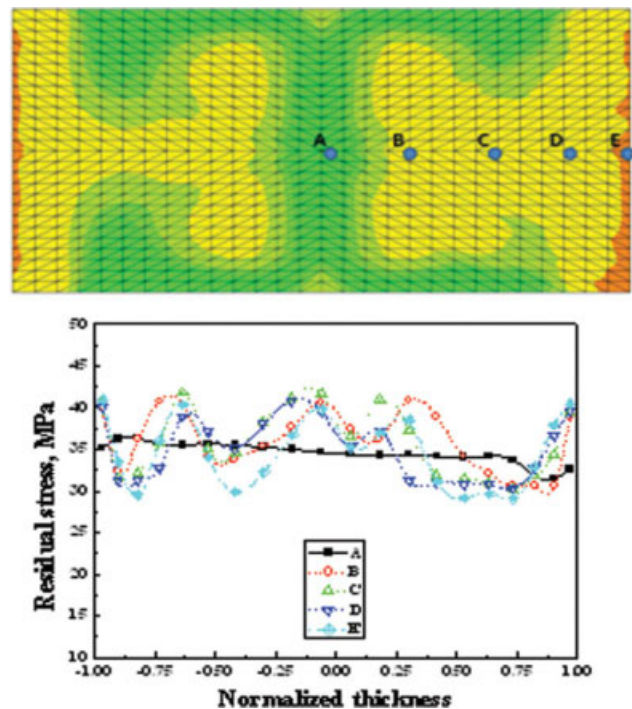


**Figure 10** Residual stress distribution of injection compression molded large-sized orthogonal stiffened plastic plate with respect to part thickness before ejection. [Color figure can be viewed in the online issue, which is available at [www.interscience.wiley.com](http://www.interscience.wiley.com).]

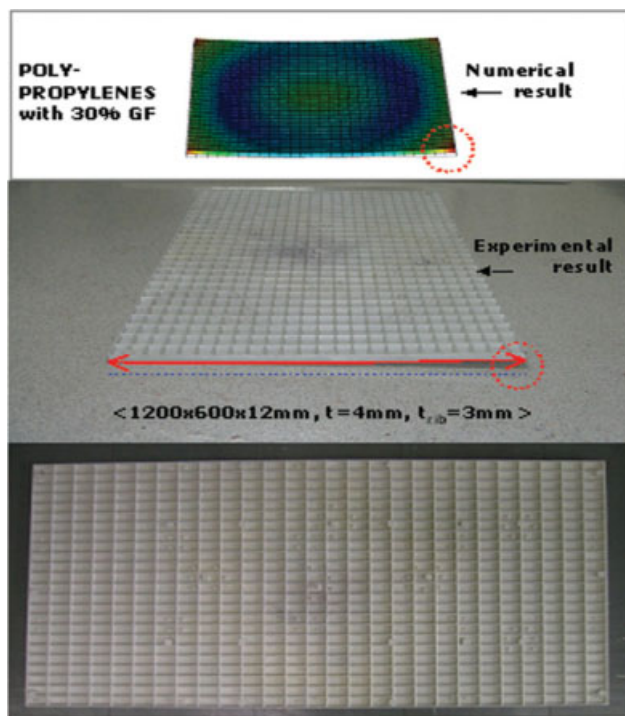


**Figure 11** Warpage of injection compression molded large-sized orthogonal stiffened plastic plate predicted by numerical analysis. [Color figure can be viewed in the online issue, which is available at [www.interscience.wiley.com](http://www.interscience.wiley.com).]

injection molding are shown in Figure 9(a) and those for the injection compression molding are illustrated in Figure 9(b). Filling of the cavity by the injection compression molding was much faster than that by the injection molding. Parallel flow path was observed at both ends of the cavity in the case of one gate system. It was expected that less warpage would occur because strength of the part was increased in the flow direction due to fiber orientation. Therefore, one gate system was selected for production of the composite plate.

Residual stress distribution of about 28–41 MPa was expected by the numerical simulation as shown in Figure 10 and the results indicated that amplitude of residual stress distribution of the injection compression molded part was smaller than that of the injection molded part. Consequently, excellent dimensional stability of the product is expected due to lower residual stresses of the injection compression molded product. When comparing between compression force for the injection compression molding and the clamp force for the injection molding, the compression force required for the large-sized orthogonal stiffened plastic plate was lower than one-tenth of the clamp force for the injection molding.

Warpage of the large-sized orthogonal stiffened plastic plate produced the injection compression

molding was obtained by experiments and numerical calculation, which is shown in Figure 11. Warpage whose magnitude was similar to the thickness of the specimen was observed, and both experimental and predicted results were in good agreement with each other. Warpage of the injection compression molded plate was much less than that of the injection molded product. Numerical analyses were carried out in this study to predict the warpage exactly for the injection molded and injection compression molded products. Warpage of the composite plate was reduced significantly by using the injection compression molding. The injection compression molding will be utilized to substitute expensive and disused wooden plates for frame materials in construction with inexpensive and recyclable polymer based composite plates.

## CONCLUSIONS

Warpage of large-sized orthogonal stiffened plastic plates that were prepared by injection molding and injection compression molding was investigated. Although warpage is inevitable due to thermal shrinkage of polymeric materials and large size of the product, the warpage was minimized by numerical prediction and experimental studies. Relatively large warpage was observed in the case of the injection molded part but small warpage of 1.5% was generated in longitudinal direction by the injection compression molding. All the numerical predictions were in good agreement with the experimental results. Compression force for the injection compression molding was only 6% of the clamp force for the injection molding. Therefore, Warpage of the injection and injection compression molded products was predicted by the numerical analysis and controlled efficiently by using the injection compression molding method.

## References

1. Chung, B. Y.; Lee, G.; Lee, H. C.; Go, S. S. *Archit Inst Korea* 2007, 23, 171.
2. Osswald, T. A.; Turng, L. S.; Gramann, P. J. *Injection Molding Handbook*; Hanser Publisher: New York, 2001.
3. Lee, S. H.; Hwang, C. J.; Kim, O. R.; Heo, Y. M. *The Warpage of Orthogonal Stiffened Structures in Injection Molding*; Polymer Processing Society 2004, ASIA/AUSTRALIA Meeting; Korea, 2004.
4. Choi, D. S.; Im, Y. T. *Compos Struct* 1999, 47, 655.
5. Lee, B. H.; Kim, B. H. *Polym Plast Technol Eng* 1995, 34, 793.
6. Lee, B. H.; Kim, B. H. *Polym Plast Technol Eng* 1997, 36, 791.
7. Huang, M. C.; Tai, C. C. *J Mater Process Technol* 2001, 110, 1.
8. Abe, T.; Tanaka, T. *Polymer Application Development Laboratory*; I. P. Co. Ltd., Asia Regional Meeting of PPS; Canada, 1991.
9. Huang, T. Y.; Chen, C. T.; Hsieh, J. R. *Internal Report of Material Industry Development Center*; Taiwan, 1993.
10. Takeo, I.; Kenzi, Y. *Internal Report of Takeo; IMURA Machinery Works Co., Ltd.*; Japan, 1992.

11. Chen, S. C.; Chen, Y. C.; Peng, H. S. *J Appl Polym Sci* 2000, 75, 1640.
12. Faupel, J. H.; Fisher, F. E. *Engineering Design: A Synthesis of Stress Analysis and Material Engineering*; Wiley: New York, 1980.
13. Isayev, A. I.; Upadhyay, R. K. *Injection and Compression Molding Fundamentals*; Marcel Dekker Inc.: New York, 1987.
14. Lee, C. C.; Castro, J. M. In *Fundamentals of Computer Modeling for Polymer Processing*; Tucker, C. L., Ed.; Hanser Publisher: New York, 1989.
15. Huebner, K. H.; Thronton, E. A. *The Finite Element Method for Engineers*; Wiley: New York, 1982.
16. Macosko, C. W. *Rheology, Principles, Measurements, and Applications*; Wiley-VCH: New York, 1994.
17. Kennedy, P. *Flow Analysis Reference Manual*; Moldflow Pty. Ltd.: Australia, 1993.
18. Santhanam, N.; Chiang, H. H.; Himasekhar, K.; Tuschak, P.; Wang, K. K. *Adv Polym Technol* 1992, 11, 77.
19. Kim, S. Y.; Kim, S. H.; Oh, H. J.; Lee, S. H.; Baek, S. J.; Youn, J. R.; Lee, S. H.; Kim, S.-W. *J Appl Polym Sci* 2009, 111, 642.
20. Kim, S. Y.; Lee, S. H.; Baek, S. J.; Youn, J. R. *Macromol Mater Eng* 2008, 293, 969.
21. Back, S. J.; Kim, S. Y.; Lee, S. H.; Youn, J. R.; Lee, S. H. *Fiber Polym* 2008, 9, 747.
22. Kim, S. Y.; Oh, H. J.; Kim, S. H.; Kim, C. H.; Lee, S. H.; Youn, J. R. *Polym Eng Sci* 2008, 48, 1840.